J. Cosmet. Sci., **56**, 297–309 (September/October 2005)

A novel method for visualizing hair lipids at the cell membrane complex: Argon sputter etching/scanning electron microscopy

YOSHINORI MASUKAWA, HIROMI SHIMOGAKI, KENJI MANAGO, and GENJI IMOKAWA, *Tochigi Research Laboratories, Kao Corporation, 2606 Akabane, Ichikai-machi, Haga, Tochigi, 321-3497 (Y.M., H.S., G.I.), and Wakayama Research Laboratories, Kao Corporation, 1334 Minato, Wakayama, Wakayama, 640-8580 (K.M.), Japan.*

Accepted for publication May 11, 2005. Based on a presentation at the 13th International Hair-Science Symposium, Potsdam, Germany, September 10–12, 2003

Synopsis

Hair lipids localized at the cell membrane complex (CMC) play a part in chemical diffusion, cell cohesion, and mechanical strength. There is no method currently available to visualize hair lipids at the CMC. We found that scanning electron microscopy (SEM) of a transversely polished hair plane followed by argon sputter etching (ASE) provides a specific characteristic image consisting of circular patterns (CP) and stitch patterns (SP) at the cortex. Both the CP and the SP are formed as convex structures and are associated with melanin granules and the CMC, respectively. While the convex formation of the CP is not affected by any treatments tested, that of the SP disappeared following treatment of hair fibers with organic solvents and reappeared following incubation of the solvent-treated hair fibers with melting lipids, which suggests that the hair lipids are responsible for the convex SP. Other treatments, such as chemical fixation, thin sectioning, and pre-/post-incubation of the hair plane, reduce or abolish the convex formation of the SP. These findings suggest that the following pathway leads to the convex formation of SP during ASE: (a) joule heat is generated on the surface by violent collisions of argon ions, (b) melting CMC lipids ooze out from the inside to the surface, and (c) CMC lipids that have oozed out are chemically changed, leading to the final convex formation of the SP. With ASE-SEM, visualization of hair lipids as convex structures of SP should enable us to characterize the fine structure and localization of hair lipids and to clarify the roles and functions of the CMC of human hair.

INTRODUCTION

The cell membrane complex (CMC) consists mainly of proteins and lipids and is distributed between cortical or cuticle cells of human hair as well as wool (1–3). The CMC

Address all correspondence to Genji Imokawa.

Purchased for the exclusive use of nofirst nolast (unknown)
From: SCC Media Library & Resource Center (library.scconline.org)

is composed of a tram-line structure including a densely stained δ-layer (proteins) sandwiched between lightly stained β-layers (lipids) on both sides (1). It has been proposed that lipids of the CMC comprise a bilayer structure, based upon the fact that lipids extracted from wool or human hair are able to form liposomes (4,5). A strong orientation of hair lipids, probably at the CMC, in planes parallel to the axis of hair fibers, has been recently shown using a microbeam synchrotron radiation diffraction technique (6). Therefore, it has been suggested that lipids of the CMC play roles in the physicochemical phenomena of hair fibers, such as chemical diffusion, cell cohesion, and mechanical strength (2,3,7–9).

Since the CMC has a thickness of approximately 25 nm (1–3), optical microscopy is not able to resolve the CMC structure. On the contrary, as transmission electron microscopy (TEM) has conventionally been used to observe the CMC (1–3), electron microscopy (which is superior in spatial resolution to optical microscopy) provides sufficient resolution to analyze the subtle structures of hair fibers. However, the β-layers in TEM images always appear as negative staining patterns, not attributable to the existence of the lipids, which implies that the β-layers do not directly reflect lipids distributed in the CMC. Although scanning electron microscopy (SEM) can clarify the fine structure of hair fibers, it is impossible to observe lipids in the CMC using SEM, even of a polished hair plane, since detection in SEM is based upon secondary electrons derived from an uneven surface. Thus, there are currently no available methods to directly visualize lipids in the CMC of hair fibers.

We have recently found that argon sputter etching-SEM (ASE-SEM) of a transversely polished hair plane provides a specific characteristic image, especially at the cortex. This finding prompted us to determine how the characteristic image on the surface of the hair plane is generated by ASE-SEM and to validate the use of ASE-SEM images in research on the microstructures of hair fibers. In this study, we have characterized ASE-SEM images of the hair plane by examining the effects of several treatments on the ASE-SEM images.

MATERIALS AND METHODS

CHEMICALS

Epon 812 resin, 25% glutaraldehyde, and osmium tetroxide were from TAAB (Reading, UK). Oleyl oleate, myristyl myristate, and isopropyl palmitate were from Kao (Tokyo, Japan), while other fats and oils were from Tokyo-Kasei (Tokyo, Japan) or Wako (Tokyo, Japan).

MATERIALS

Scalp hair fibers were obtained from a healthy Japanese volunteer, aged 28 years. The volunteer had never subjected her hair to any chemical treatments such as perming or coloring, except for shampooing and conditioning. The hair fibers were washed with n-hexane for 5 min and then were cut to *ca.* 1 cm prior to preparation for ASE-SEM.

Purchased for the exclusive use of nofirst nolast (unknown)
From: SCC Media Library & Resource Center (library.scconline.org)

ASE-SEM OBSERVATION

The 1-cm hair fiber was embedded in resin, and then a transversely polished resin-embedded hair block was exposed to ASE for SEM observation. The Epon 812 resin containing the hair fiber was polymerized in an oven. Rough trimming of each hair block with a glass knife was followed by the careful polishing of a transverse hair plane with a diamond knife (MT6740, DiATOME Ltd., Switzerland). The carefully polished hair block was placed in the target position for ASE in an Hitachi Ion Sputter E-1030 (Hitachinaka, Japan) connected to an argon cylinder. The specimen was then etched under a pressure of 6 to 7 Pa, a current of 6 mA, a voltage of 0.3 kV, a working distance of 30 mm, and a time of 360 sec, as shown in Figure 1. The etched specimen was coated with a *ca.* 5-nm layer of Pt-Pd using the same instrument (Hitachi Ion Sputter E-1030). Observation of the polished hair plane was performed using an FE-SEM Hitachi S-4300 SEM under an accelerating voltage of 5 kV. For observation of thin sections, 1-μm-thick sections were cut with a sapphire knife while 90-nm ultra-thin sections were cut with a diamond knife. ASE was then performed for the hair sections on a cover glass using the same procedures and the same conditions as those used for the polished hair planes.

COMPARISON OF ASE-SEM IMAGES WITH TEM IMAGES

The transversely polished resin-embedded hair block was prepared according to the procedures described above. An ultra-thin section of the block was cut with a diamond knife, and then was stained with uranyl acetate and lead citrate (3). The ultra-thin sections were observed with a TEM (Hitach H-7000) under an accelerating voltage of 75 kV. If a clear TEM image was obtained, another polished hair plane of the remaining block was examined by ASE-SEM. In case of an unclear TEM image, further ultra-thin

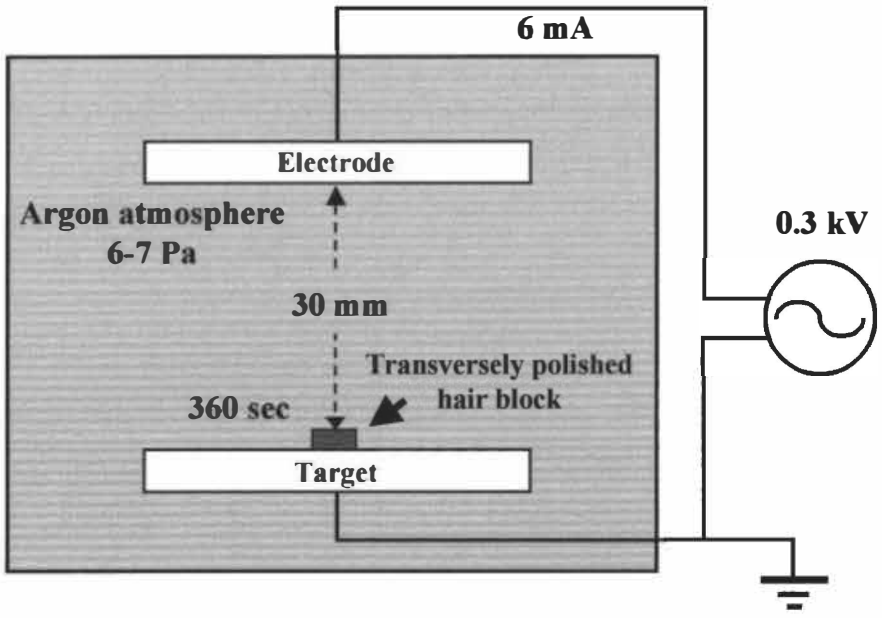

Figure 1. Schematic diagram of the instrument used for ASE in this study.

Purchased for the exclusive use of nofirst nolast (unknown)
From: SCC Media Library & Resource Center (library.scconline.org)

sections were cut and subsequent TEM observations were continued until a clear TEM image were recorded.

TREATMENTS OF HAIR FIBERS AND POLISHED HAIR PLANES

Treatments of hair fibers were as follows: (a) immersion of hair fibers into CH_3Cl/CH_3OH/water (v/v/v, 18:9:1) at room temperature for 24 hr, (b) immersion of solvent-treated hair fibers into melting lipids at 80°C for 24 hr, and (c) chemical fixation with glutaraldehyde and osmium tetroxide. The polished hair planes were observed with ASE-SEM followed by pre- and post-incubation with ethanol or n-hexane. Pre- and post-incubations refer to incubations with the solvent just before ASE and just after ASE, respectively.

OBSERVATION OF THE POLISHED HAIR PLANE BY OPTICAL MICROSCOPY

Optical microscopic images of polished hair planes were observed with a Microwatcher (Mitsubishi Chemical, Tokyo, Japan) via a reflection mode. The IR (infrared) spectrum of the polished hair plane was measured with an IR microscope (Spectrum One, Perkin Elmer, UK) using an ATR (attenuated total reflection) mode.

RESULTS

CHARACTERISTICS OF ASE-SEM IMAGES OF THE HAIR PLANE

SEM images of transversely polished hair planes with or without ASE are shown in Figure 2. In the SEM images without ASE, as used conventionally, the hair plane can be visualized only as the even surface, and therefore, micro-three-dimensional structures of the cuticle and the cortex in the hair plane could not be observed (Figure 2a). In contrast, when ASE treatment was performed on the hair plane prior to SEM observation, microstructures of the cuticle and the cortex became distinct with a characteristic pattern at the cortex (Figure 2b). The magnified image of the cortex revealed that it was mainly composed of two types of structure, circular-shaped ones and slender thread-shaped ones, designated here as circular patterns (CP) and stitch patterns (SP), respectively. When several parameters associated with the efficiency of ASE, such as pressure, voltage, current, working distance, and treatment time, were characterized, we found that of all parameters tested, pressure most strongly affected ASE-SEM images of the hair plane, and that a pressure of 6 to 7 Pa is required for an optimal ASE-SEM image.

A comparison of ASE-SEM images at the tilting angle of 45 degrees toward the primary electron beam with images at no tilting angle demonstrated that both CP and SP are convex structures in the surrounding plane (Figure 3). In order to determine the intra- or intercellular localization of CP and SP in the cortex, TEM images of ultra-thin sections and ASE-SEM images in the adjacent plane were observed. In a representative TEM image (Figure 4a), there are densely stained melanin granules and the lightly stained CMC. A comparison of each TEM image with the adjacent ASE-SEM image

Purchased for the exclusive use of nofirst nolast (unknown)
From: SCC Media Library & Resource Center (library.scconline.org)

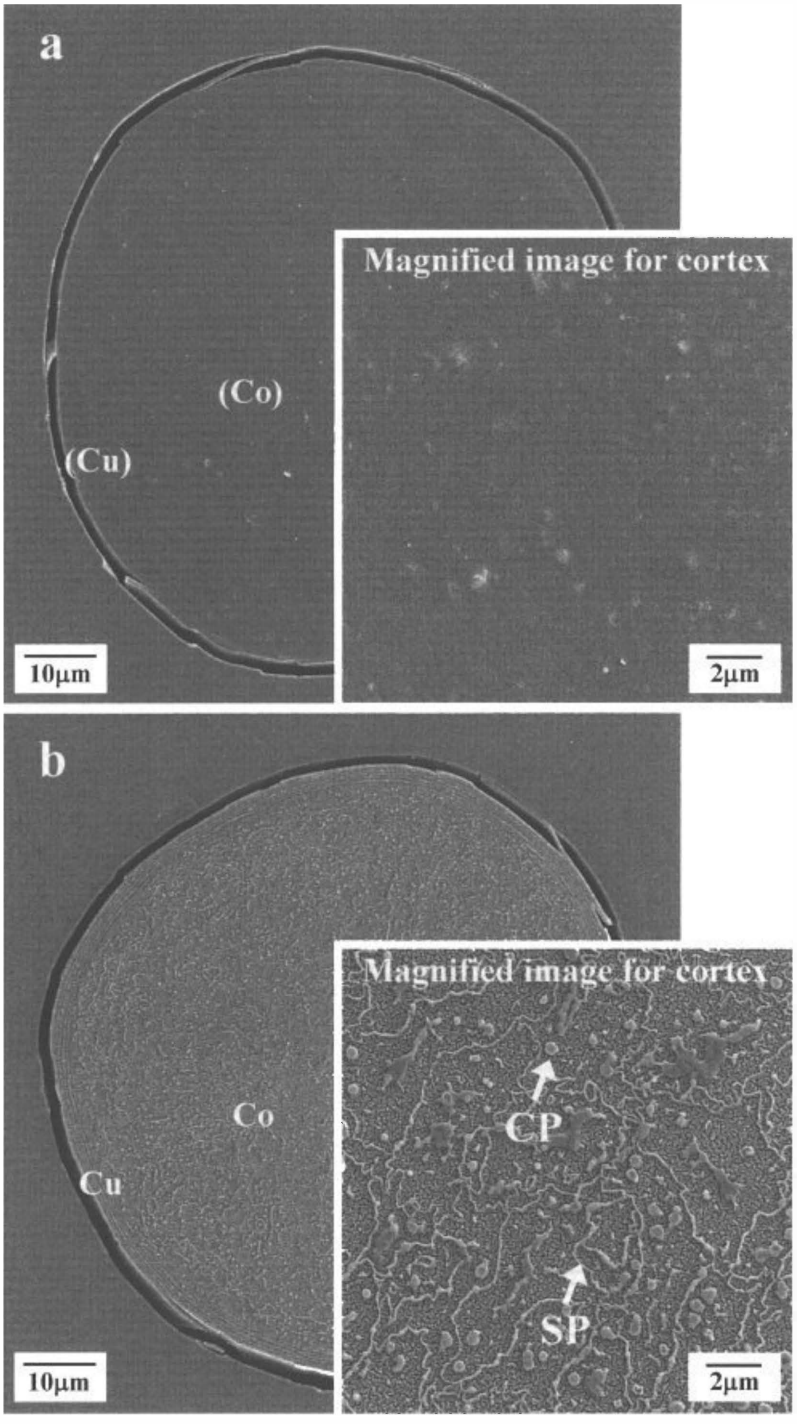

Figure 2. SEM images of transversely polished hair planes without ASE (a) and with ASE (b). ASE-SEM image (b) includes a circular pattern (CP) and a stitch pattern (SP) in the magnified image of the cortex. Cu: cuticle. Co: cortex.

Purchased for the exclusive use of nofirst nolast (unknown)
From: SCC Media Library & Resource Center (library.scconline.org)

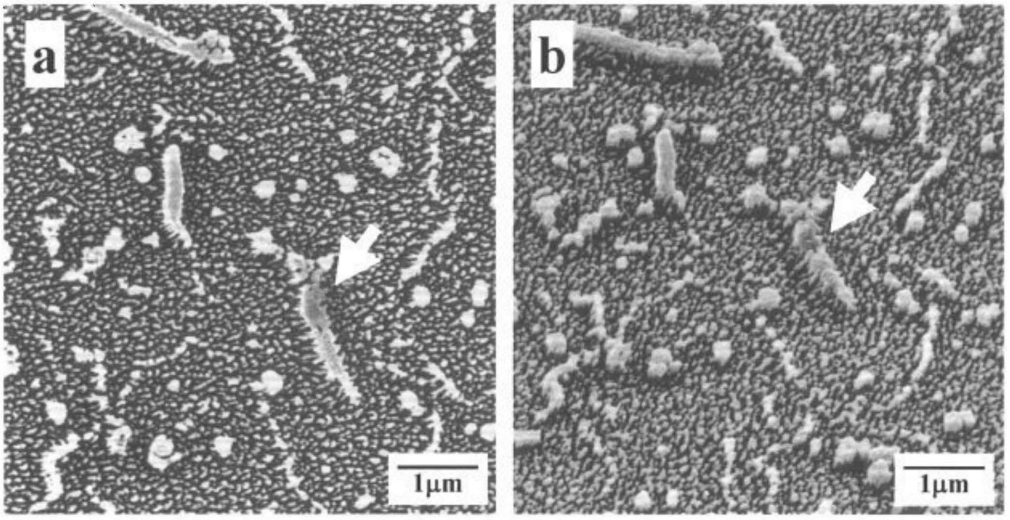

Figure 3. ASE-SEM images of transversely polished hair planes at no tilting angle (a) and at a tilting angle of 45 degrees (b) toward the primary electron beam. The arrow in each image shows the same region.

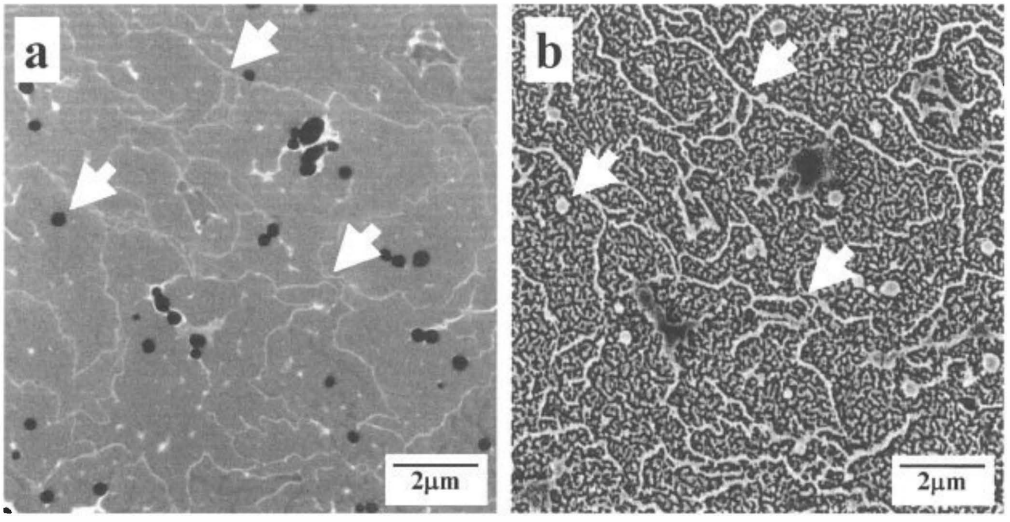

Figure 4. A TEM image (a) of a transversely ultra-thin section of a hair fiber and an ASE-SEM image (b) of the adjacent hair plane. The arrows in each image show the same regions.

suggests that CP and SP in ASE-SEM images correspond to melanin granules and the CMC, respectively (Figure 4).

EFFECTS OF HAIR TREATMENTS ON ASE-SEM IMAGES

The effects of various treatments of hair fibers on ASE-SEM images of the polished hair planes were then examined. When a hair fiber was treated with a mixture of $CHCl_3$/CH_3OH/water (v/v/v 18:9:1) for 24 hr at room temperature, SP but not CP disappeared in the ASE-SEM images (Figure 5b; compare with the untreated control, Figure 5a). On

Purchased for the exclusive use of nofirst nolast (unknown)
From: SCC Media Library & Resource Center (library.scconline.org)

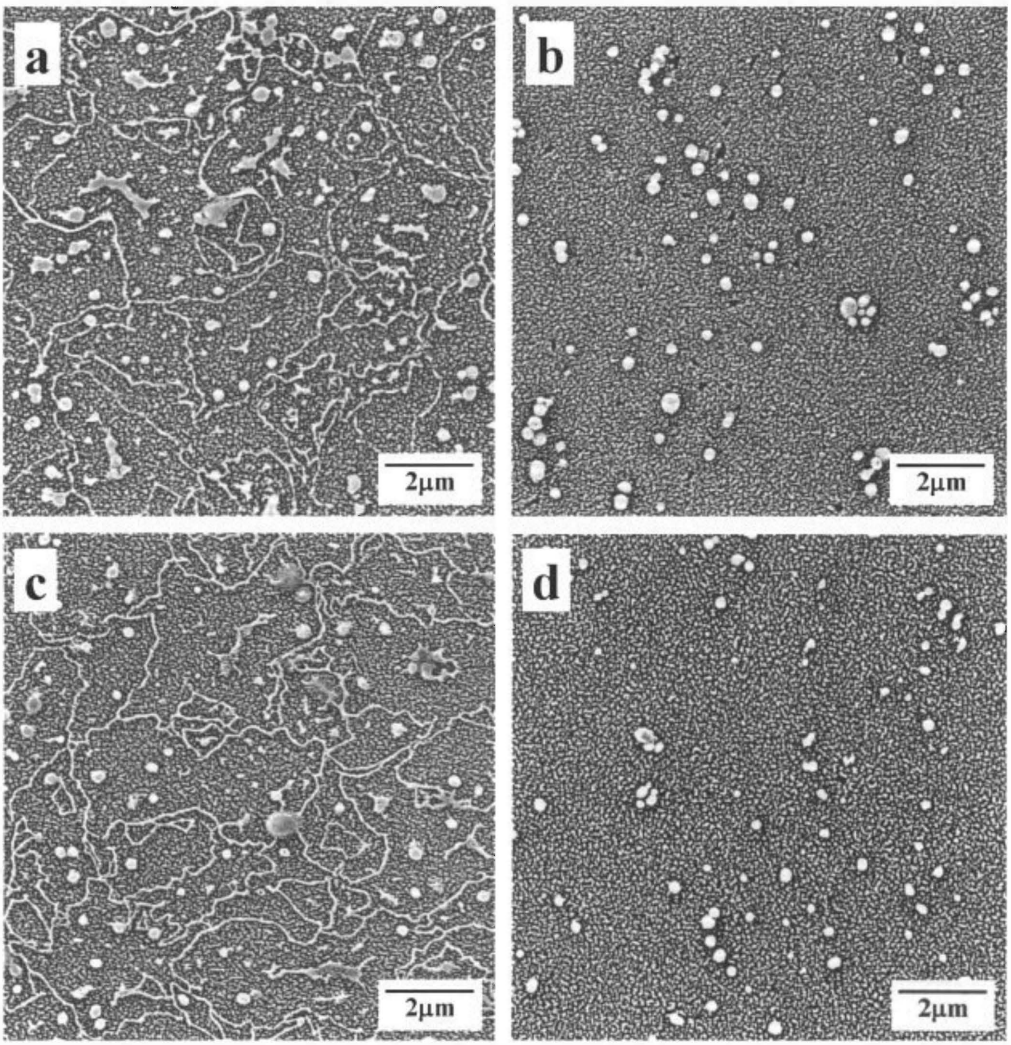

Figure 5. ASE-SEM images of transversely polished hair planes following various treatments of the hair fibers. a: An untreated hair fiber (control). b: A hair fiber treated with $CHCl_3/CH_3OH$/water 19:9:1 for 24 hr. c: A solvent-treated hair fiber incubated with a melting lipid mixture (squalene/oleyl olate/triolein/oleic acid [wt 10:30:10:50]) at 80°C for 24 hr (a solvent-treated hair corresponds to that treated with $CHCl_3/CH_3OH$/water 19:9:1 for 24 hr). d: A solvent-treated hair fiber incubated with melting triolein at 80°C for 24 hr.

the other hand, when solvent-treated hair fibers were further incubated with a melting lipid mixture (squalene/oleyl olate/triolein/oleic acid [wt 10:30:10:50], which is a model of hair lipids) for 24 hr at 80°C, SP reappeared while CP remained unchanged (Figure 5c). Images similar to that shown in Figure 5c were also obtained by incubation with other lipids that melt at 80°C, such as C_{12}-C_{18} fatty acids, myristyl myristate, oleyl oleate, and isopropyl palmitate (data not shown). In contrast, SP did not reappear following treatment with triolein (Figure 5d).

The effects of chemical fixation of hair fibers on ASE-SEM images of the polished hair

Purchased for the exclusive use of nofirst nolast (unknown)
From: SCC Media Library & Resource Center (library.scconline.org)

planes were also studied. Whereas a single fixation of hair fibers with glutaraldehyde only or a double fixation with glutaraldehyde and osmium tetroxide did not change the appearance of CP in the ASE-SEM images, SP became poorly defined following double fixation (Figure 6). This implies that chemical fixation with osmium tetroxide but not glutaraldehyde affects CMC to reduce the convex structures of SP in the ASE-SEM images.

Figure 7 shows ASE-SEM images of thin sections of a hair fiber. In 1-μm-thin sections, both CP and SP were present (Figure 7a), although SP became slightly shorter and thicker and were distinct from SP in the usual hair plane (e.g., compare with Figure 2). Some cracks in this ASE-SEM image seemed to have occurred during its preparation. On the other hand, in 90-nm ultra-thin sections, CP were present with no changes, but SP disappeared completely (Figure 7b). It seems likely that SP in the ASE-SEM images disappear in 90-nm ultra-thin sections, which suggests that underlying structures more than 90 nm in thickness are essentially required for the convex formation of SP.

ASE-INDUCED CHANGES IN THE HAIR PLANE

The effects of incubating the hair plane with organic solvents were studied next. Pre- and post-incubation with ethanol or n-hexane were used just before ASE and just after ASE. In the ASE-SEM images, pre-incubation of the hair plane with ethanol for a few minutes abolished SP whereas CP were not affected (Figure 8a). On the other hand, post-incubation with ethanol affected neither CP nor SP even when treated longer than 60 min (Figure 8-b). Similar results were obtained for pre- or post-incubation with n-hexane (data not shown).

Optical microscopic images of the polished hair planes with or without ASE demonstrated that ASE elicited a remarkable change from a transparent colorless plane to a

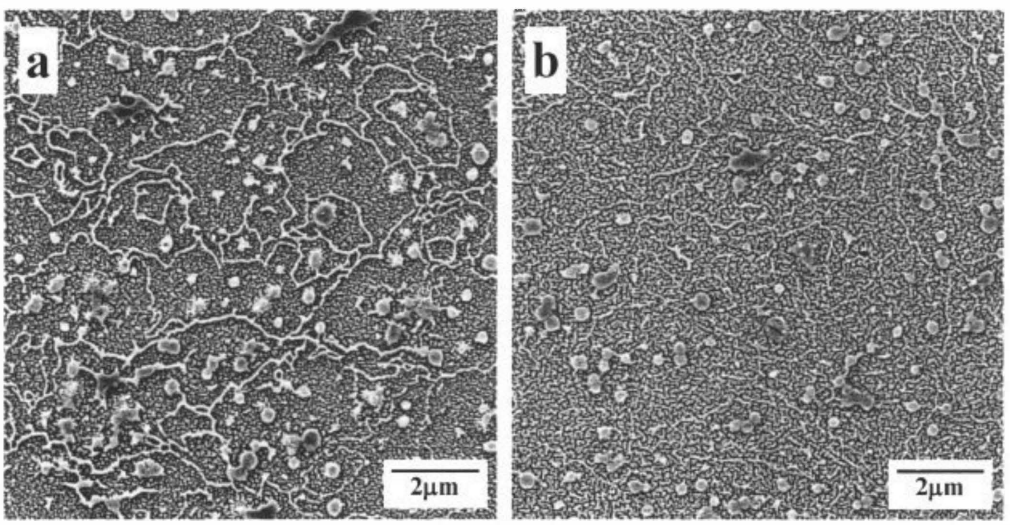

Figure 6. ASE-SEM images of transversely polished hair planes following single chemical fixation of hair fibers with glutaraldehyde (a) and double chemical fixation with both glutaraldehyde and osmium tetroxide (b).

Purchased for the exclusive use of nofirst nolast (unknown)
From: SCC Media Library & Resource Center (library.scconline.org)

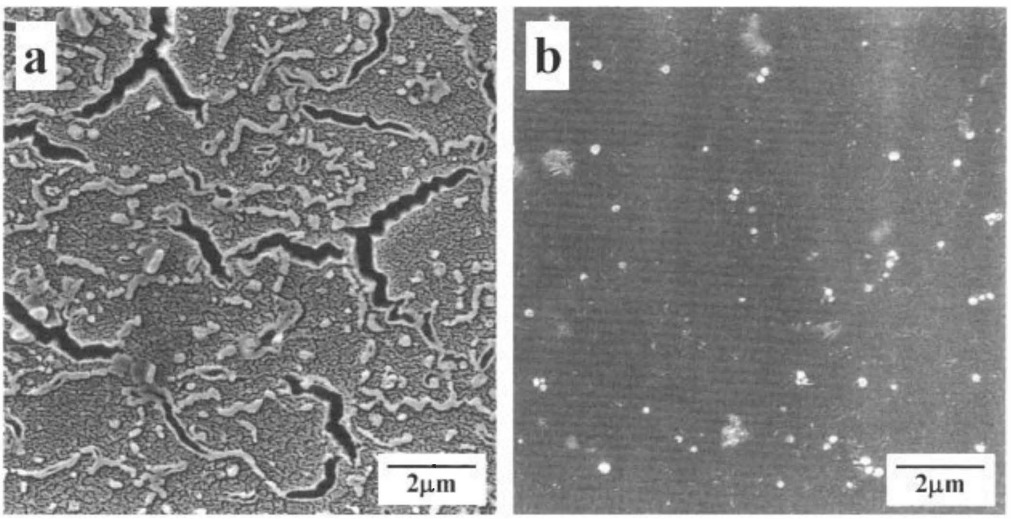

Figure 7. ASE-SEM images of transverse thin hair sections of 1-μm thickness (a) and 90-nm thickness (b).

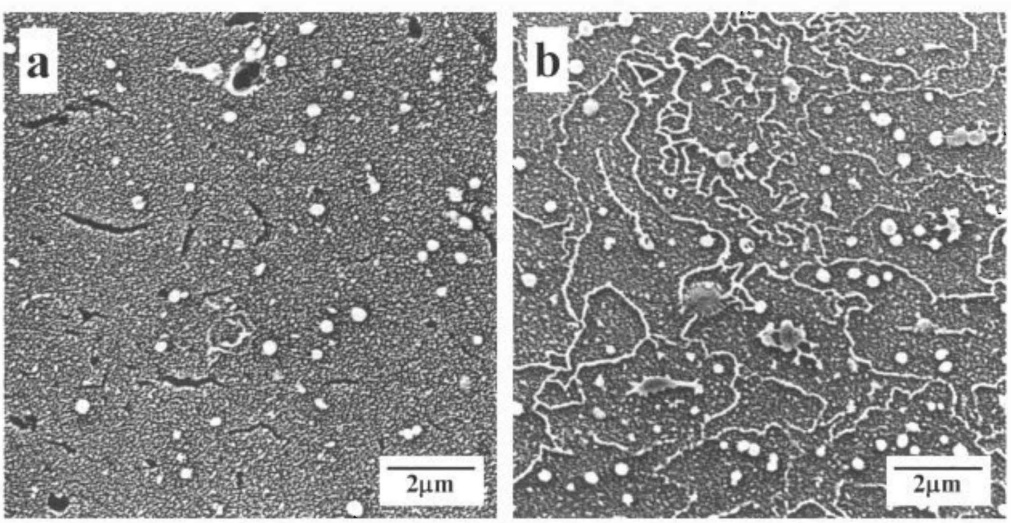

Figure 8. ASE-SEM images of transversely polished hair planes incubated with ethanol. Pre-incubation of the hair plane for 2 min (a) and post-incubation of the hair plane for 60 min (b) were performed. Pre- or post-incubation represents treatments just prior to ASE or just after ASE, respectively.

black opaque one, except for melanin granules and the medulla (Figure 9). Thus, ASE seems to generate a black hair plane with high reproducibility (n = 4). Analysis with microscopic IR/ATR was also tried. This technique revealed that there was a difference in absorption at *ca.* 1740 cm^{-1} with or without ASE, with a high reproducibility (n = 4), indicating a stronger absorption in the hair plane treated with ASE than that without ASE.

DISCUSSION

Etching-SEM based on plasma etching (PE) and sputter etching (SE) have been used to

Purchased for the exclusive use of nofirst nolast (unknown)
From: SCC Media Library & Resource Center (library.scconline.org)

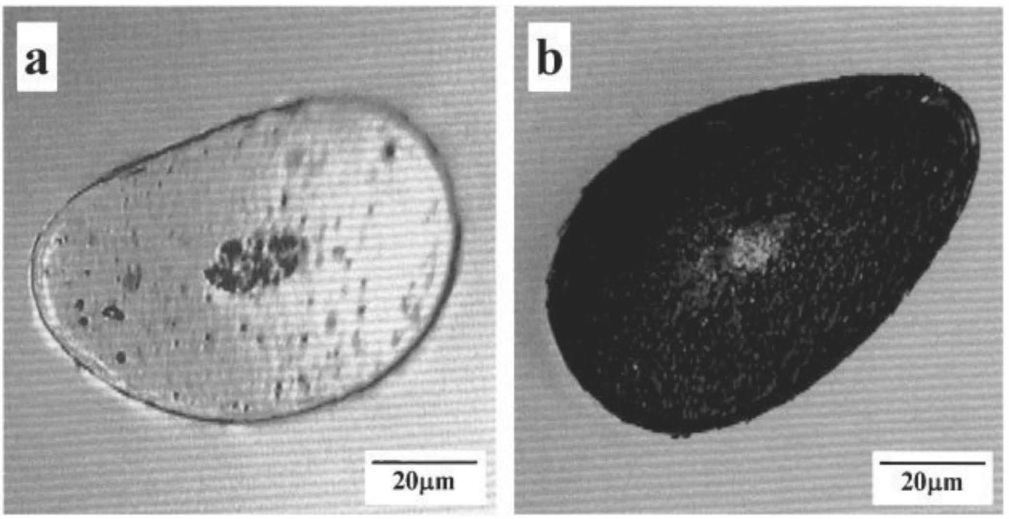

Figure 9. Optical microscopic images of transversely polished hair planes without ASE (a) and with ASE (b).

observe the surfaces or the insides of various materials (10–19). Although both PE and SE belong to the same dry etching system, their principles differ. The PE technique is based upon the principle that a chemically reactive gas plasma generated by radiofrequency or by a microwave electrical discharge can readily react with surface molecules on the target, resulting in the production of volatile molecules (10,13–18), and oxygen gas has been generally used for oxygen plasma etching (OPE). In contrast, the SE technique is based upon the principle that gas ions generated by glow discharge in a low vacuum collide with surface molecules on the target, resulting in sputtering atoms or molecules at the surface (11,12,19), and argon gas has been generally used for ASE. Although there have been studies on the internal structure of hair fibers observed by OPE-SEM (14,15), no corresponding study has been reported using SE (ASE)-SEM to the best of our knowledge.

In this study, ASE-SEM images of transversely polished hair planes have been characterized for the first time. We found that the ASE-SEM images are distinct from OPE-SEM images (14,15) in their three-dimensional structures. Thus, in ASE-SEM, there are highly characteristic images consisting of circular-shaped structures (CP) and slender thread-shaped ones (SP) with convexity in the cortex of transversely polished hair planes. A comparison of ASE-SEM images with TEM images revealed that these convex structures correspond to melanin granules and the CMC, respectively, while melanin granules and the CMC in the OPE-SEM images have been reported to be convex and concave, respectively (14,15). Based upon the morphological differences in the CMC between those techniques, it would be of considerable interest to determine what components contribute to the convex formation of SP during ASE. Our observation that SP but not CP disappear following treatment of hair fibers with $CHCl_3/CH_3OH$/water strongly suggests that convex SP are mainly comprised of hair lipids of the CMC since treatment with $CHCl_3/CH_3OH$/water is a typical solvent for removing lipids (20). The suggestion that SP is comprised of hair lipids also supports other experiments in which incubation of the solvent-treated hair fibers with lipids restores the convex formation. Thus, incu-

Purchased for the exclusive use of nofirst nolast (unknown)
From: SCC Media Library & Resource Center (library.scconline.org)

bation with fatty acids or wax esters elicits the reappearance of SP, although triolein does not have that effect, which may result from its inability to penetrate into the hair fiber due to its large molecular size.

In the mechanism involved in the convex formation of CP, there is a simple etching mechanism as reported previously in several cases (10–19): convex CP are formed due to the great difference between the slower etching of melanin granules and the faster etching of the surrounding proteins. This mechanism is also corroborated by our observations that no treatments (such as incubation with solvent, chemical fixation, and thin sectioning) affected the appearance of CP in the hair plane by ASE.

As for the mechanism involved in the convex formation of SP, it is of considerable interest to characterize how hair lipids can generate convex structures during ASE. Our findings that the convex SP disappeared after chemical fixation with osmium tetroxide and in 90-nm-thick ultra-thin sections cannot be explained in terms of a simple etching mechanism. Our observation using chemical fixation of hair fibers revealed that fixation with osmium tetroxide, but not with glutaraldehyde, markedly diminished the convex structures of SP. Since osmium tetroxide fixes both proteins and lipids while glutaraldehyde fixes only proteins, it is likely that the existence of mobile lipids is essential for the convex formation of SP during ASE. Another observation using thin sectioning of hair fibers demonstrated that there is no convex formation of SP in ASE-SEM images using 90-nm-thick ultra-thin sections. This result suggests that hair structures with a minimal thickness are essentially required for the convex formation of SP during ASE. In addition, our results using optical microscopy revealed that ASE elicits a remarkable change from a transparent colorless plane to a black opaque one, implying that heat is generated in the hair plane during ASE. We also showed that SP formation is not affected by post-incubation with ethanol, whereas it is completely abolished following pre-incubation with ethanol, which indicates an alteration of the chemical status of hair lipids during ASE. Based upon the above findings, the mechanism(s) involved in the convex formation of SP at the CMC during ASE might be as depicted in Figure 10: (a) joule heat is generated on the surface by violent collisions of argon ions, (b) melting hair lipids at the CMC ooze out from the inside of the hair plane to the surface, and (c) lipids that have oozed out from the CMC are chemically changed by the additional collision energy of argon ions, leading to the final convex formation of SP. The chemical change in hair lipids might be associated with complex reactions such as the polymerization of lipids or the covalent binding of lipids with proteins during ASE.

Although the convex SP do not seem to be distinct etching structures, it is plausible that the convexity of SP in ASE-SEM images can be used as a good indicator to visualize the fine structure and localization of hair lipids. In OPE-SEM observations for internal structures of a hair fiber (14,15), Swift (14) stated that the "cell membrane is etched at far greater rates due to the lowest sulfur content" according to the principle of OPE, which results in the concave structures of the CMC in the surrounding proteins. Although the location of the CMC in a hair fiber is detectable by OPE-SEM, it is not sufficient to directly visualize the fine structure of hair lipids. This is because the concave structure of the CMC is responsible for the lower content of sulfur within the proteins, but is not relevant to the hair lipids. On the other hand, although conventional TEM also allows the observation of microstructures, including the β-layers and δ-layer of the CMC in a hair fiber, the structures of the β-layers are not directly responsible for the hair lipids. In our experience, even if the hair lipids are lost, the β-layers of the CMC in TEM

Purchased for the exclusive use of nofirst nolast (unknown)
From: SCC Media Library & Resource Center (library.scconline.org)

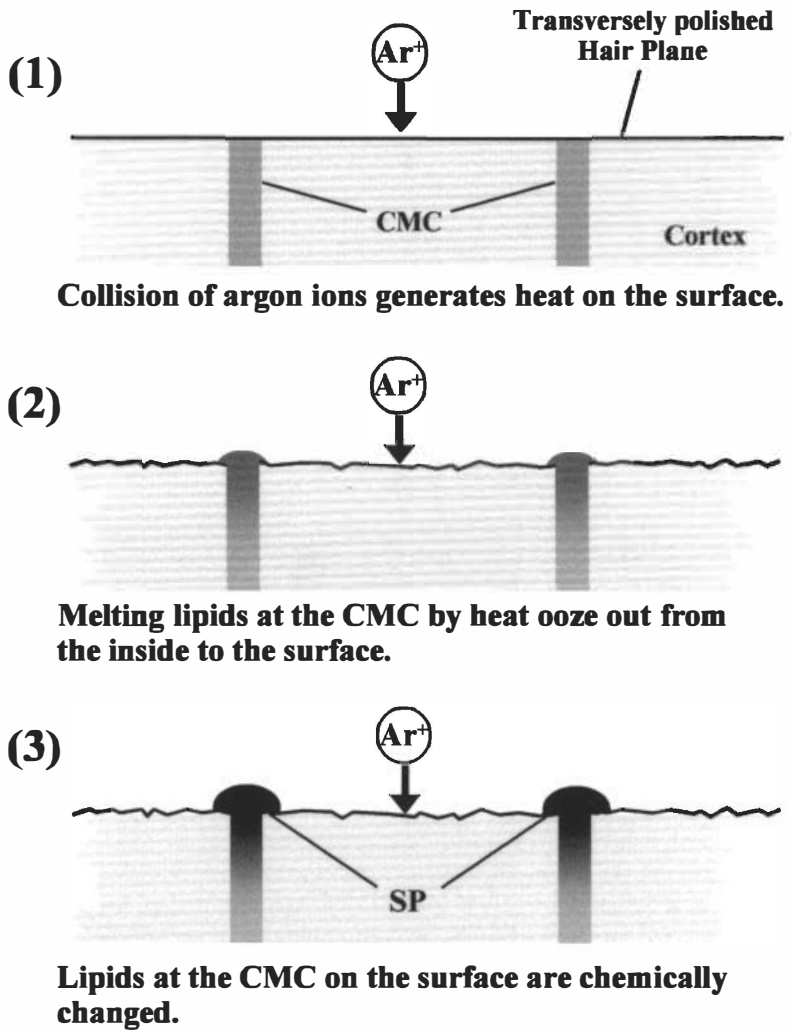

Figure 10. Schematic diagram of the mechanism underlying the convex formation of SP at the CMC on the surface of the hair plane during ASE.

images are detectable as staining patterns similar to that of hair fibers with higher contents of hair lipids.

CONCLUSIONS

This study explored a novel method using ASE-SEM to observe the convex CP of melanin granules and the convex SP of CMC in transversely polished hair planes. With ASE-SEM, visualization of hair lipids as convex structures of SP should enable us to characterize the fine structure and localization of hair lipids and to clarify the role(s) and function(s) of the CMC of hair.

ACKNOWLEDGMENTS

We express our cordial gratitude to Dr. Kouichi Nakamura and Dr. Katsumi Kita for

Purchased for the exclusive use of nofirst nolast (unknown)
From: SCC Media Library & Resource Center (library.scconline.org)

their invaluable discussions and guidance in this study. Our sincere thanks are also due to Ms. Miho Suzuki for technical support in the SEM studies.

REFERENCES

(1) J. A. Swift and A. W. Holmes, Degradation of human hair by papain. Part II. Some electron microscope observations, *Text. Res. J.,* **35,** 1014–1019 (1965).
(2) J. D. Leeder, The cell membrane complex and its influence on the properties of the wool fibre, *Wool Sci. Rev.,* **63,** 3–35 (1986).
(3) S. Naito, T. Takahashi, M. Hattori, and K. Arai, Histochemical observation of the cell membrane complex of hair, *Sen-I Gakkaishi,* **48,** 420–426 (1992).
(4) A. Körner, S. Petrovic, and H. Höcker, Cell membrane lipids of wool and human form liposomes, *Text. Res. J.,* **65,** 56–58 (1995).
(5) L. Coderch, A. de la Maza, A. Pinazo, and J. L. Parra, Physicochemical characteristics of liposomes formed with internal wool lipids, *J. Am. Oil Chem. Soc.,* **73,** 1713–1718 (1996).
(6) L. Bertrand, J. Doucet, A. Simionovici, G. Tsoucaris, and P. Walter, Lead-revealed lipid organization in human hair, *Biochim. Biophys. Acta,* **1620,** 218–224 (2003).
(7) K. Nishimura, M. Nishino, Y. Inaoka, Y. Kitada, and M. Fukushima, Interrelationship between the hair lipids and the hair moisture, *J. Cosmet. Sci. Soc. Jap.,* **13,** 134–139 (1989).
(8) V. Sideris, L. A. Holt, and I. H. Leaver, A microscopical study of the pathway for diffusion of rhodamine B and octadecylrhodamine B into wool fibers, *J. Soc. Dyers Colorists,* **106,** 131–135 (1990).
(9) M. Philippe, J. C. Garson, P. Gilard, M. Hocquaux, G. Hussler, F. Leroy, C. Mahieu, D. Semeria, and G. Vanlerberghe, Synthesis of 2-N-oleoylamino-octadecane-1,3-diol: A new ceramide highly effective for the treatment of skin and hair, *Int. J. Cosmet. Sci.,* 17, 133–146 (1995).
(10) R. S. Thomas and J. R. Hollahan, Use of chemically-reactive gas plasmas in preparing specimens for scanning electron microscopy and electron probe microanalysis, *Scanning Electron Microsc.,* **1,** 83–92 (1974).
(11) T. Fujita, T. Nagatani, and A. Hattori, A simple method of ion-etching for biological materials. An application to blood cells and spermatozoa, *Arch. Histol. Jap.,* **36,** 195–204 (1974).
(12) T. Nagatani and M. Yamada, Application of ion-etching for biological materials, *The Cell (Tokyo),* **7,** 136–142 (1975).
(13) W. J. Humphreys and W. G. Henk, Ultrastructure of cell organelles by scanning electron microscopy of thick sections surface-etched by an oxygen plasma, *J. Microsc.,* **116,** 255–264 (1979).
(14) J. A. Swift, A technique for the rapid examination of the gross internal structure of mammalian keratin fibres, *J. Text. Inst.,* **3,** 170–174 (1980).
(15) S. Seta, H. Sato, M. Yoshino, and S. Miyasaka, SEM/EDX analysis of inorganic elements in human scalp hairs with special reference to the variation with different locations on the head, *Scanning Electron Microsc.,* **1,** 127–140 (1982).
(16) R. Sellamuthu, J. Barkanic, E. Karwacki, and R. Jaccodine, Application of SEM and XPS in plasma etching of single crystal silicon, *Microbeam Anal.,* **21,** 653–655 (1986).
(17) A. C.-M. Yang, R. D. Allen, and T. C. Reiley, Evaluation of particle dispersion in polymer solids by oxygen plasma etching, *J. Appl. Polym. Sci.,* **46,** 757–762 (1992).
(18) G. Danev, E. Spassova, and K. Popova, Morphology of thin polyimide films, *Thin Solid Films,* **228,** 301–303 (1993).
(19) T. Nagato, Y. Hisanaga, D. Shimizu, and T. Fujiwara, Scanning electron microscopy of ion-etched epoxy resin sections and its application to three-dimensional reconstruction, *Electron Microsc.,* **36,** 131–134 (2001).
(20) E. G. Bligh and W. J. Dyer, A rapid method of total lipid extraction and purification, *Can. J. Biochem. Physiol.,* **37,** 911–917 (1959).

Purchased for the exclusive use of nofirst nolast (unknown)
From: SCC Media Library & Resource Center (library.scconline.org)